Electric Power System Stabilization by Virtual Inertia and Fast Grid Frequency Support of Grid-Following Virtual Synchronous Generator

Teppei Fujita[1], Ryuto Shigenobu[1], Masakazu Ito[1], Norikazu Kanao[2], and Hitoshi Sugimoto[2]
[1] University of Fukui, Fukui, Japan
[2] Hokuriku Electric Power Company, Toyama, Japan
Email: fujita.teppei@pws.fuee.u-fukui.ac.jp; {lute; itomasa}@u-fukui.ac.jp; n.kanao@rikuden.co.jp; sugimoto.hitoshi@rikuden.co.jp

***Abstract*—The Virtual Synchronous Generator (VSG) can give virtual inertia and imitate primary control of the synchronous generator. This paper focuses on grid-following (GFL) type VSG for easy parallel operation compared to voltage source inverter. The grid frequency support of GFL-VSG can be achieved by controlling active power output using frequency deviation. However, this control causes the delay because of feedback for the virtual inertia. This paper proposes the GFL-VSG with the parallel installation of the governor and swing equation to reduce the delay. The numerical simulation was carried out to verify its effect and grid frequency support of the proposed GFL-VSG. The result shows that grid frequency support by GFL-VSG is faster compared with the conventional method, and the gate frequency is more stable with multiple several VSGs.**

***Index Terms*—Grid-following inverter, virtual synchronous generator, virtual inertia, system frequency support**

I. Introduction

For a sustainable society and environment, massive introduction of Renewable Energy (RE), such as photovoltaic systems and wind power systems, is required [1]-[2]. The RE is connected to the power system by inverters [3]-[5]. At this time, the active and reactive power of the inverter can be controlled by adjusting current by following the voltage and the phase angle of the grid voltage reference. This type of control is called a grid-following (GFL) inverter control. Power electronics devices such as inverters do not have kinetic motion in electromagnetic energy conversion because they have no rotating parts like a synchronous generator (SG). Consequently, high system non-synchronous penetration (SNSP) by the massive introduction of REs reduces the electric system's inertia due to replacing the SG. This could lead to instability conditions compared to SG-dominated conventional systems [6]-[8].

An alternative method is required to increase inertia and system stability instead of conventional SG. Thus, virtual synchronous generator (VSG) control [9] that emulates inertia and damping function has been proposed to provide SG characteristics by an inverter. The VSG control can be divided into two types of inverter control, GFL inverter and the grid-forming (GFM) inverter. The GFM inverter controls the voltage magnitude and its phase. Therefore, GFM has been categorized as a voltage-controlled inverter and has been reported in [10], [11]. The small-signal model of GFM type VSG was derived in [12]. Comparison of VSG and droop function for P-ω control on GFM inverter was provided by [13], and high performance of VSG function regarding mitigation of frequency fluctuation was reported. The authors in [14] proposed altering the inertia value of VSG function on GFM inverter by considering its virtual angular velocity. This method can also be used to suppress the frequency and power oscillations. In the work of literature [15], the behavior of multiple GFM having VSG function and paralleled with SG was investigated in a microgrid, and the authors mentioned that GFM can provide similar characteristics of replaced SG.

However, the interaction of GFM inverters has not been investigated under high SNSP. Also, the GFM can provide frequency, however, control conflict and lack of synchronous ability by the generated frequency from GFM control are concerned on high SNSP conditions. In contrast, GFL inverters are generally installed as an inverter for REs in a real system with a synchronous function such as a phase locked loop. Thus, GFL inverter can provide VSG function without conflict, or inner disturbance, even under any power system, e.g., GFM inverters dominating grid. Also, GFL type VSG has low obstacles compared to GFM control systems because GFL control is already highly penetrated conventionally.

The virtual inertia function can be achieved in both GFM and GFL, and the advantages and disadvantages of each inverter type have been discussed. On the other hand, the VSG function is not only virtual inertia, but also primary control is essential to maintain the stability of the grid for the both inverter types. Therefore, this paper develops a VSG function that can simultaneously achieve virtual inertia and primary control. In this paper, GFL inverter type is assumed. The primary control function is

Manuscript received October 16, 2021; revised December 28, 2021; accepted January 20, 2022.
Corresponding author: Teppei Fujita (email: fujita.teppei@pws.fuee.u-fukui.ac.jp).

doi: 10.18178/ijeetc.11.4.277-283

equivalent to the governor-free operation mode of the SG. It plays an important role in frequency control by changing the active power output command according to the frequency deviation. This paper also proposes a configuration that consists of the governor and swing equation which operate independently and parallel to each other. This configuration is for the fast system frequency support function. This high-speed operation characterizes the proposed method, because the primary control does not through control blocks of swing equation part for inertia. In order to verify the effectiveness of the proposed GFL-VSG, numerical simulation is examined. In addition, the penetration ratio of the GFL-VSG is discussed.

II. GRID-FOLLOWING VSG MODEL

The general structure of a GFL type VSG is shown in Fig. 1. The VSG function is achieved by applying the swing equation of SG virtually at the *P-ω* control. The GFL consists of an impedance model for calculating the current reference, a *P-ω* controller imitated the swing equation, and a *Q-E* controller carrying out the automatic voltage regulator (AVR) function. Then, the pulse width modulation (PWM) input signal is generated from the current control block. In Fig. 1, L_f and C_f are filter inductor and filter capacitor. i_s and i_g are inverter current and grid current, respectively. v_f and v_g are LC filter voltage and grid voltage, respectively. Note that the DC voltage source is assumed to be an ideal DC source, therefore the DC power capacity is not discussed in this paper.

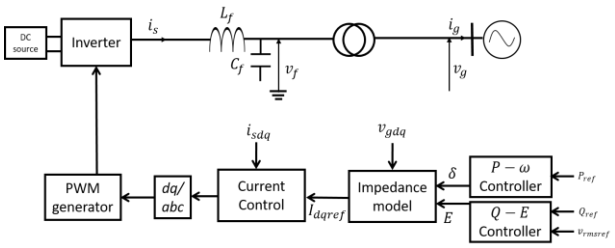

Fig. 1. GFL-VSG configuration.

A. Impedamce Model for GFL-VSG

The impedance model imitates the relation that exists between the internal electromotive force (EMF) and the terminal voltage in SG. This relation can be used to calculate the current reference. The current reference equations [16] are as follows:

$$i_{\text{dref}} = \frac{r}{r^2+x^2}\left(E\cos\delta - v_{\text{gd}}\right) + \frac{x}{r^2+x^2}\left(E\sin\delta - v_{\text{gq}}\right) \quad (1)$$

$$i_{\text{qref}} = \frac{r}{r^2+x^2}\left(E\sin\delta - v_{\text{gq}}\right) - \frac{x}{r^2+x^2}\left(E\cos\delta - v_{\text{gd}}\right) \quad (2)$$

where r and x are virtual armature resister and virtual reactance, respectively, E is the virtual internal EMF, δ is the internal phase angle. δ and E are obtained from *P-ω* controller and *Q-E* controller. The detailed impedance model was given in [16].

B. P-ω Controller and Virtual Inertia

The inner phase angle is derived from the system electric phase angle and VSG virtual phase angle. Equation (3) indicates the inner phase angle:

$$\delta_{\text{vsg}} = \theta_{\text{vsg}} - \theta_{\text{grid}} \quad (3)$$

where θ_{vsg} is VSG virtual phase angle, and θ_{grid} is the electrical system phase angle. The electric system phase angle is obtained from the system frequency. To obtain VSG virtual phase angle, the virtual angular velocity is calculated by the swing equation of SG. By applying the swing equation, the distributed generator can imitate the inertial response. Applying the swing equation:

$$2H\frac{d\omega^*_{\text{vsg}}}{dt} = P^*_{\text{ref}} - P^*_{\text{out}} - D(\omega^*_{\text{vsg}} - \omega^*_{\text{grid}}) \quad (4)$$

the virtual phase angle is calculated by

$$\frac{d\theta_{\text{vsg}}}{dt} = \omega^*_{\text{vsg}}\omega_{\text{base}} \quad (5)$$

where P_{ref} and P_{out} are the active power reference and the VSG output, respectively. The asterisk * represents per unit (p.u.) value. H and D represent the virtual inertia constant and the virtual damping coefficient. ω^*_{vsg}, and ω_{grid} are the VSG virtual angular velocity, grid angular velocity. ω_{base} is base angular velocity and is used to unit conversion.

The *P-ω* controller is shown in Fig. 2.

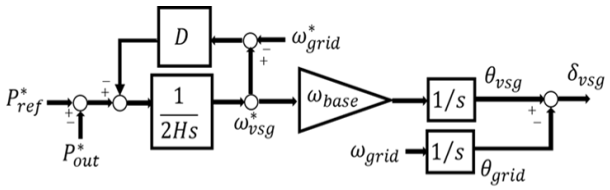

Fig. 2. *P-ω* controller.

C. Q-E Controller

Virtual internal EMF E is obtained from the *Q-E* controller. *Q-E* controller equation [16] is given by

$$E = \left[\left(Q_{\text{ref}} - Q_{\text{out}}\right)D_q + v_{\text{rmsref}} - v_{\text{rms}}\right]\left(k_p + \frac{k_i}{s}\right) \quad (6)$$

Q-E controller simply imitates the excitation system of SG. The PI regulator regulates the voltage signal. *Q-E* controller is represented in Fig. 3. Q_{ref} and Q_{out} are the reactive power reference and the VSG reactive power output, respectively. D_q is the voltage droop coefficient. v_{rmsref} and v_{rms} are voltage reference and grid voltage, respectively.

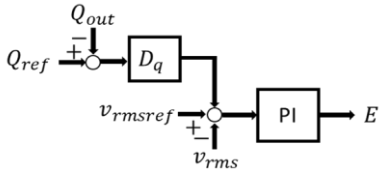

Fig. 3. *Q-E* controller.

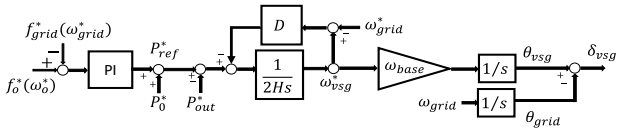

Fig. 4. Conventional governor model (governor model (a)).

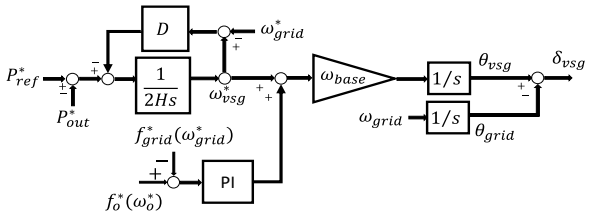

Fig. 5. Proposed governor model (governor model (b)).

D. Proposed Governor Model for Grid-Support

Grid support function can be achieved by applying the model of free-governor operation to GFL-VSG. As shown in Fig. 4, the governor model can change the VSG active power reference according to the deviation between the system frequency and the reference system frequency, such as the droop characteristic of SG. However, the active power output has a significant delay caused though virtual inertia block by precisely model imitation. Meanwhile, inverter control block can be improved flexibly, and no need to imitate physical phenomenon precisely. Namely, the grid-support function does not need to go through the inertia block part. Hence, the topology can divide inertia and primary control parts and connect parallelly, which is proposed in this paper as a fast system frequency support function. As shown in Fig 5, this proposed topology calculates the virtual angular velocity from the swing equation and the frequency deviation of the system frequency and the reference frequency. This control can ignore delay caused by the virtual inertia constant term. In this study, PI control for frequency deviation was adopted to restore system frequency to its reference frequency by GFL-VSG.

III. GFL-VSG Response

The virtual inertia response and proposed grid-support function of the primary control function are simulated in this section.

A. Virtual Inertia Response of GFL-VSG

A test case simulation was conducted to evaluate the inertia effect by GFL-VSG. Inertia affects the rate of change of frequency (RoCoF) such as load change and fault condition. To evaluate the inertia effect, the test case was assumed as shown in Fig. 6. As shown in Table I, the test case assumed that the SG is replaced by VSG that can output comparably, where SG#1 can adjust the amount of active power for lack of it in both cases. The test case disturbance was 10% (0.7 MW) load increase. In the simulation, as the VSG model is explained in Section II, the parameter of VSG is shown in Table II.

TABLE I: CONDITION OF TEST CASE

Case	P_{load} [MW]	P_{SG2} [MW]	$P_{DG(VSG)}$ [MW]
1	7.000	2.000	0
2	7.000	0	1.841

TABLE II: VSG PARAMETER

Parameters name	Variables	Values
filter inductor	L_f	3[mH]
filter capacitor	C_f	5[μF]
virtual damping coefficient	D	30
voltage droop coefficient	D_q	0.05
PI gain of Q-E controller	k_p	0.05
PI gain of Q-E controller	k_i	0.05
base angular velocity	ω_{base}	377[rad/s]

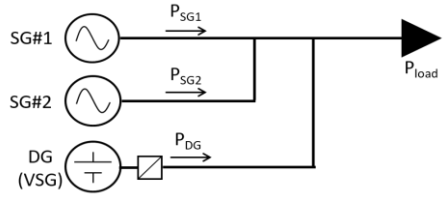

Fig. 6. Configuration of test case.

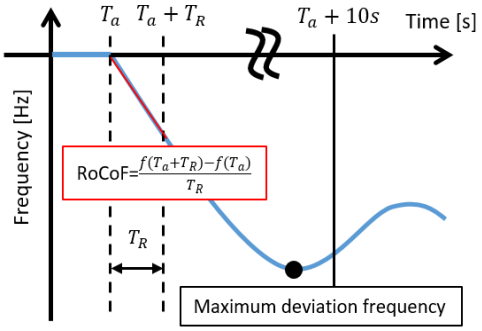

Fig. 7. Overview of RoCoF and maximum deviation frequency.

To evaluate the inertia effect by VSG, SG#1 has a governor function but SG#2 and VSG have no governor function. RoCoF and maximum deviation frequency between disturbance timing and at after 10 seconds are used as the evaluation index. RoCoF is calculated by

$$\mathrm{RoCoF}\left[\mathrm{Hz/s}\right]=\frac{f(T_a+T_R)-f(T_a)}{T_R} \tag{7}$$

where f is frequency, T_a is the time at which the event happened, T_R is a time window for measuring RoCoF value, and the width of T_R is set 500 ms in this paper. RoCoF and maximum deviation frequency are shown in Fig. 7.

The result of the test case is shown in Fig. 8 and 9. Fig. 8 shows the active power output of VSG, Fig. 9 represents the system frequency. From this result, the additional active power output is supplied from when the disturbance happened to 20 seconds by virtual inertia constant value at Fig. 8. The inertia function is achieved because the active power output of VSG with the active power output of SG#2 (Fig. 8) shows a similar output response corresponding to the same inertia value. Also, frequency response shows a similar result with case 1(SG case) and case 2 (VSG case). The evaluation indexes are summarized in Table III. It can be confirmed that RoCoF and maximum deviation frequency had similar result. Therefore, GFL-VSG can give the inertia function as similarly as SG to the electric system.

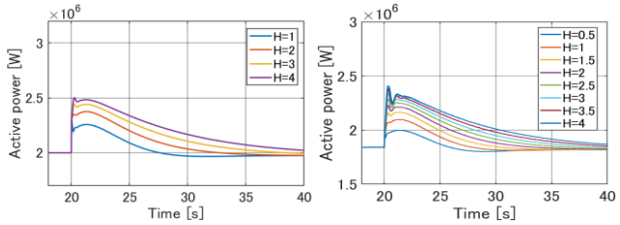

(a) (b)

Fig. 8. Active power output: (a) SG#2 (Case1) and (b) VSG (Case2).

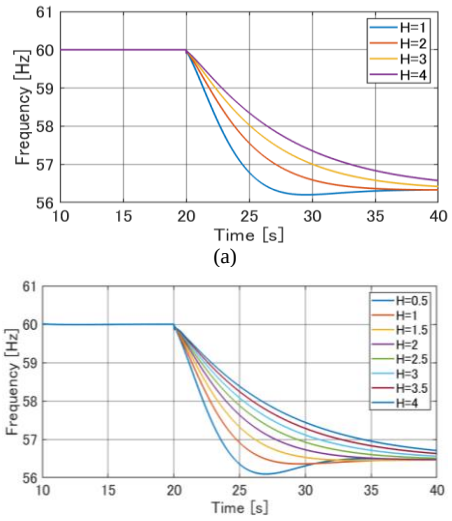

(a)

(b)

Fig. 9. Frequency: (a) Case 1 and (b) Case 2

TABLE III: EVALUATION INDEXES

Index	RoCoF[Hz/s]	Maximum deviation of frequency (20~30[s]) [Hz]
SG#2(*H*=4[s])	-0.3440	57.3563
SG#2(*H*=3[s])	-0.4110	57.0066
SG#2(*H*=2[s])	-0.5120	56.5947
SG#2(*H*=1[s])	-0.6830	56.2044
VSG(*H*=4.0[s])	-0.3634	57.4385
VSG(*H*=3.5[s])	-0.3902	57.2826
VSG(*H*=3.0[s])	-0.4360	57.1116
VSG(*H*=2.5[s])	-0.4814	56.9235
VSG(*H*=2.0[s])	-0.5428	56.7270
VSG(*H*=1.5[s])	-0.6126	56.5274
VSG(*H*=1.0[s])	-0.7044	56.3572
VSG(*H*=0.5[s])	-0.8224	56.0929

B. Grid-support by GFL-VSG with Proposed Tolopogy

To evaluate the effectiveness of the proposed governor model of VSG, the test case that is the same case as Section III A was used. GFL-VSG used two types of governor model, conventional governor model (a) and governor model (b) using proposed topology. In this simulation, all SG models have a governor. The threshold of VSG's governor model is 59.7Hz. RoCoF and maximum deviation frequency between disturbances to 10 seconds were used as evaluation index too.

The frequency of the test case is shown in Fig. 10, and active power outputs are shown in Fig. 11. From this result, the frequency of the system that consists of SG only (case 1) is not restored to the reference frequency (60Hz). On the other hand, we confirmed that the frequency of the system that is introduced to the VSG governor functioned model can restore the frequency back to its reference frequency.

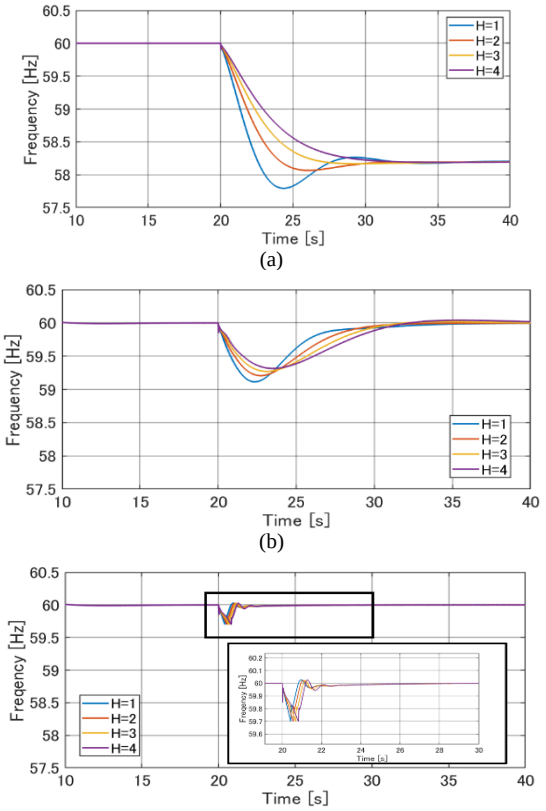

(a)

(b)

(c)

Fig. 10. Frequency: (a) Case1, (b) Case2 (Governor model (a)), and (c) Case2 (Governor model (b)).

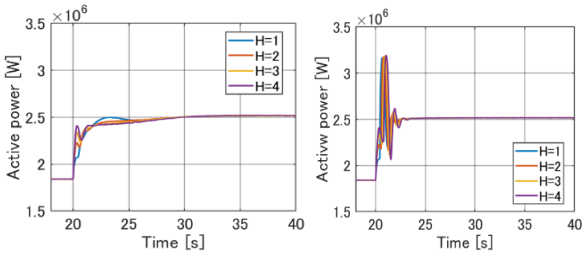

(a) (b)

Fig. 11. VSG Active power output: (a) Case2 (Governor model (a)) and (b) Case2 (Governor model (b)).

As shown in Fig. 10 (b), when the virtual inertia constant is larger than 3s, the frequency of the system consisted of GFL-VSG under the governor model (a) become larger than the reference frequency. Thus, we confirmed that the conventional governor model (a) causes delay. On the other hand, the maximum deviation of frequency is about 59.7 Hz and the system frequency is restored to reference frequency faster regardless of virtual inertia constant, when GFL-VSG governor uses proposed topology (governor model (b)) because the inertia constant is avoided. Table IV shows the evaluation indices. Compared RoCoF on the proposed topology function with the conventional governor model, RoCoF result is similar. Therefore, the virtual response is similar to the proposed topology and the conventional method. However, we confirmed that the active power output of VSG with proposed topology (governor model (b)) oscillates largely. From this verification, the proposed GFL-VSG can provide a fast grid-support function compared with the conventional method.

TABLE IV: EVALUATION INDEXES

Index	RoCoF[Hz/s]	Maximum deviation of frequency (20~30[s]) [Hz]
VSG(a)(H=4[s])	-0.3648	59.3121
VSG(a)(H=3[s])	-0.4468	59.2677
VSG(a)(H=2[s])	-0.5434	59.2038
VSG(a)(H=1[s])	-0.6920	59.1100
VSG(b)(H=4[s])	-0.3646	59.6986
VSG(b)(H=3[s])	-0.4360	59.6990
VSG(b)(H=2[s])	-0.5480	59.6986
VSG(b)(H=1[s])	-	59.6986

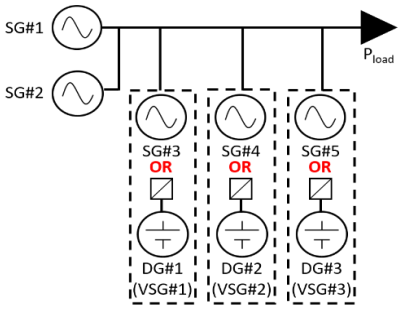

Fig. 12. System configuration.

TABLE V. SIMULATION SCENARIO

Scenario	A	A'	B	C	D
SG#1	✓	✓	✓	✓	✓
SG#2	✓	✓ no GF	✓	✓	✓
SG#3	✓	✓ no GF	✓	✓	
SG#4	✓	✓ no GF	✓		
SG#5	✓	✓ no GF			
VSG#1			✓	✓	✓
VSG#2				✓	✓
VSG#3					✓

A' is same as A but the SG#2 to #5 does not have the governor-free operation.

IV. EVALUATION OF SYSTEM STABILITY AT DIFFERENT INTEGRARION LEVELS OF GFL-VSG

The performance of frequency restoration using the proposed method is described in section III. This section provides a simulation of GFL-VSG to evaluate the proposed method and system response. The test scenario assumed an intensive penetration rate for the future SNSP power system network. The system configuration of the test scenario is shown in Fig. 12. The load in this system was 10MW. In this simulation scenario, GFL-VSG replaced SG in the system one by one, as shown in Table V, and the disturbance was assumed to be 10 % (1 MW) load increase. Then, the active power command of an SG without SG#1 and a GFL-VSG was 2MW (SG#1 adjusted the amount of active power). Note in Scenario A, all SGs except SG#1 without and with the governor-free operation are simulated. For all generators' such as SG and GFL-VSG, rated capacity and inertia constant were 10MW and 2s, respectively. Besides, parameter and PI coefficient are set to the same value on all GFL-VSGs.

Fig. 13 and Fig. 14 show the system frequency and SG outputs including several losses and VSG outputs, respectively. From Fig. 13, the system frequency does not entirely restore due to scenario A, which consists of SG only, though system frequency is stable compared with no free-governor operation. This system frequency could be due to an inadequate supply of power such as steam and water for losing rotational kinetic energy by inertia response in this simulation.

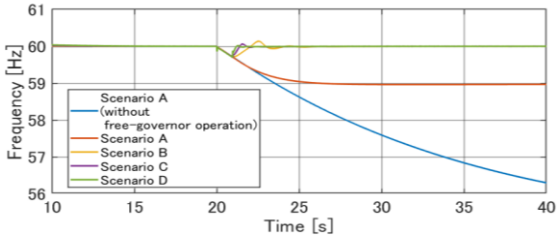

Fig. 13. Frequency.

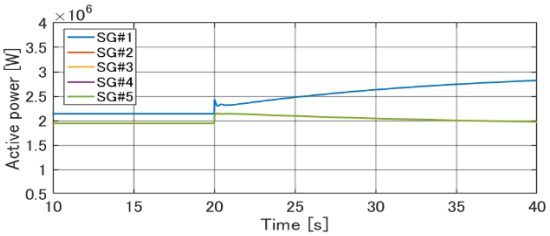

(a) Scenario A (without free-governor operation)

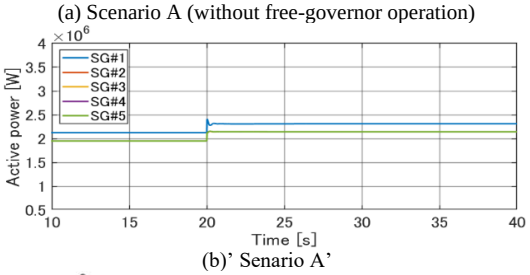

(b)' Senario A'

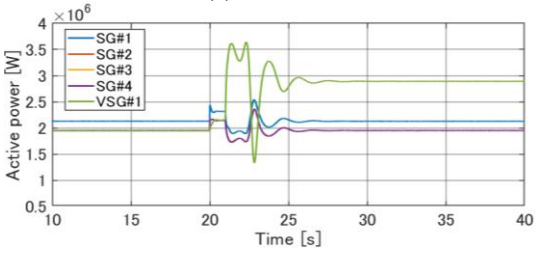

(c) Scenario B

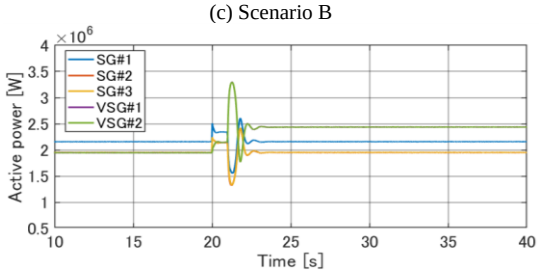

(d) Scenario C

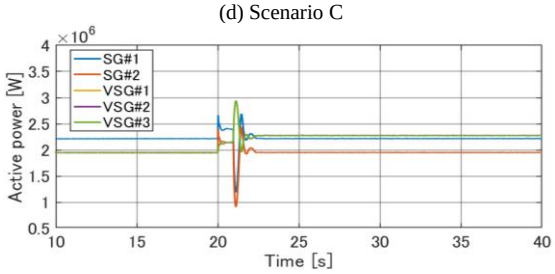

(e) Scenario D

Fig. 14. Active power output.

On the other hand, the scenarios containing the proposed GFL-VSG show that the system frequency could get fast restoration and the same inertia response as SG due to no loss of rotational kinetic energy caused by load sharing of GFL-VSG. Furthermore, we confirmed that the extensive penetration of the proposed GFL-VSG led the system to be more stable. These reasons are due to

the increase in the total active power of the VSGs immediately after the disturbance. Also, it can be seen that the load sharing amount of the active power output is the same in several GFL-VSGs as shown in Fig. 14. From this verification, the high penetration of the proposed GFL-VSG has the potential to stabilize the power system.

V. Conclusion

This paper focuses on GFL-VSG to compensate for the reduction of system inertia and primary control by the high SNSP rate. This paper proposed GFL-VSG with a governor function which can provide fast grid frequency support without delay caused by feedback control for the virtual inertia. Moreover, numerical simulations considering introduction scenarios of GFL-VSG were carried out. As a result, system stability had been improved more by increasing interconnecting rate of GFL-VSG. The required capacity of GFL-VSG to provide virtual inertia and grid support will be evaluated in future works.

Conflict of Interest

The authors declare no conflict of interest

Author Contributions

The first author created models, conducted validation and wrote draft. The second author investigated, design methodology and supervised. The third author supervised and constructed draft. The forth author and the fifth author discussed this research as a collaborative research.

References

[1] H. X. Li, D. J. Edwards, M. R. Hosseini, and G. P. Costin, "A review on renewable energy transition in Australia: An updated depiction," *Journal of Cleaner Production*, vol. 242, January 2020.

[2] U. Zafar, T. Ur Rashid, A. A. Khosa, M. S. Khalil, and M. Rashid, "An overview of implemented renewable energy policy of Pakistan," *Renewable and Sustainable Energy Reviews*, vol. 82, pp. 654-665, February 2018.

[3] A. Q. Al-Shetwi, M. Z. Sujod, M. A. Hannan, M. A. Abdullahd, A. S. Al-Ogaili, and K. P. Jern, "Impact of inverter controller-based grid-connected pv system in the power quality," *Int. Journal of Electrical and Electronic Engineering & Telecommunications*, vol. 9, no. 6, pp. 462-469, November 2020.

[4] G. S. Babu, U. K. Choudhury, G. TulasiramDas, and A. M. Kumar, "An economical approach of designing a three phase grid tied inverter for solar applications," *Int. Journal of Electrical and Electronic Engineering & Telecommunications*, vol. 1, no. 1, pp. 30-42, October 2012.

[5] R. Kumaresan and I. Gnanambal, "Seven level inverter with single DC source interconnected photovoltaic system," *Int. Journal of Electrical and Electronic Engineering & Telecommunications*, vol. 5, no. 2, pp. 1-15, April 2016.

[6] M. Reza, D. Sudarmadi, F. A. Viawan, W. L. Kling, and L. van der Sluis, "Dynamic stability of power systems with power electronic interfaced DG," in *Proc. IEEE PES Power Systems Conference and Exposition*, 2006, pp. 1423-1428.

[7] A. Ulbig, T. S. Borsche, and G. Andersson, "Impact of low rotational inertia on power system stability and operation," *IFAC Proceedings*, vol. 47, no. 3, pp. 7290-7297, 2014.

[8] P. Tielens and D. Van Hertem, "The relevance of inertia in power systems," *Renewable and Sustainable Energy Reviews*, vol. 55, pp. 999-1009, March 2016.

[9] J. Jongudomkarn, "Multivariable model predictive control for a virtual synchronous generation-based current source inverter," *Int. Journal of Electrical and Electronic Engineering & Telecommunications*, vol. 10, no. 3, pp. 196-202, May 2021.

[10] S. D'Arco, J. Are Suul, and O B. Fosso, "A virtual synchronous machine implementation for distributed control of power converters in SmartGrids," *Electric Power System Research*, vol. 122, pp. 180-197, May 2015.

[11] P. Hesse, D. Turschner, and H. P. Beck, "Micro grid stabilization using the virtual synchronous machine (VISMA)," *Renewable Energies and Power Quality*, vol. 1, no. 7, pp. 676-681, 2009.

[12] H. Wu, X. Ruan, D. Yang, *et al.*, "Small-signal modeling and parameters design for virtual synchronous generators," *IEEE Trans. on Industrial Electronics*, vol. 63, no. 7, pp. 4292-4303, July 2016.

[13] J. Liu, Y. Miura, and T. Ise, "Comparison of dynamic characteristics between virtual synchronous generator and droop control in inverter-based distributed generators," *IEEE Trans. on Power Electronics*, vol. 31, no. 5, pp. 3600-3611, May 2016.

[14] J. Alipoor, Y. Miura, and T. Ise, "Power system stabilization using virtual synchronous generator with alternating moment of inertia," *IEEE Journal of Emerging and Selected Topics in Power Electronics*, vol. 3, no. 2, pp. 451-458, June 2015.

[15] X. W. Yan, S. Y. A. Mohamed, D. X. Li *et al.*, "Parallel operation of virtual synchronous generators and synchronous generators in a microgrid," *Journal of Engineering*, vol. 16, pp. 2635-2642, March 2019.

[16] Y. Hirase, K. Abe, K. Sugimoto, and Y. Shindo, "A grid-connected inverter with virtual synchronous generator model of algebraic type," *Electrical Engineering in Japan*, vol. 184, no. 4, pp. 10-21, Sep. 2013.

Teppei Fujita received his the B.Sc. degree in Electrical, Electronic and Computer Engineering from University of Fukui, Japan, in 2020. He is currently pursuing the M.Sc degree in System and Infrastructure Engineering for Safe and Sustainable Society. His current research interests are virtual synchronous generator.

Ryuto Shigenobu received the B.Eng. and M.Eng. degrees in electrical and electronics engineering from the University of the Ryukyus, Japan, in 2015 and 2017, and the Ph.D. degree from the University of the Ryukyus in 2019. His research includes optimization methods and electric power systems. He has been an Assistant Professor in the Department of Electrical and Electronics Engineering at the University of Fukui, Japan.

Masakazu Ito was born in Tokyo, Japan in 1978. He is an Associate Professor at the Faculty of Engineering, the University of Fukui, Japan. He organizes a Power System Laboratory and researches on 3 topic groups; research on renewable energy technologies; power network research; and Life-Cycle Assessment and Ecological footprint. He earned his Ph.D. from the Tokyo University of Agriculture and Technology. He started as an assistant professor at the Tokyo Institute of Technology, and then became a JSPS Overseas Research Fellow researching at the CEA at INES in France and associate professor at the Waseda University.

Norikazu Kanao was born in Toyama, Japan on September 19, 1959. He received the B.Sc. and M.Sc. degrees in electrical engineering from Nagoya University, Japan, in 1982 and 1984, and the Ph.D. degree from the University of Fukui, Japan in 2006. Dr. Kanao joined Hokuriku Electric Power Company, Toyama, Japan, in 1984. He is an advisory manager in charge of the Innovation Laboratory of the company and works on the study of power system analysis.
He is a senior member of the Institute of Electrical Engineering of Japan.

Hitoshi Sugimoto was born in Toyama, Japan on November 18, 1965. He received the B.Sc. degree in electrical engineering from Niigata University, Japan, in 1988 and the Ph.D. degree from Shibaura Institute of Technology, Japan in 2002. Dr. Sugimoto joined Hokuriku Electric Power Company, Toyama, Japan, in 1988. He is a deputy general manager in the Innovation Laboratory of the company and works on the study of the lightning protection for power distribution systems and customer's facilities.
He is a member of the Institute of Electrical Engineering of Japan, and the Institute of Electrical Installation Engineering of Japan.